COMPARISON OF OIL RECOVERY FOR SIX NANOFLUIDS IN BEREA SANDSTONE CORES

Katherine R. Aurand, Gunnar Sie Dahle, and Ole Torsæter
Norwegian University of Science and Technology, Trondheim, Norway

This paper was prepared for presentation at the International Symposium of the Society of Core Analysts held in Avignon, France, 8-11 September, 2014

ABSTRACT

Recent studies have shown that using nanofluids (nanoparticles suspended in fluids) in a way similar to water flooding shows promise as a new enhanced oil recovery (EOR) technique. The objective of this study was to determine the optimum nanoparticle morphology and particle size for EOR while gaining insight into the mechanisms driving the system.

The tests were conducted at ambient conditions using core flooding analysis. Water wet, high permeability (avg. K ≈ 362 mD) Berea sandstone cores (length 13 cm and diameter 3.8 cm) were used for the testing. Hydrophilic nanoparticles and nano-structured particles were suspended in a synthetic North Sea water solution at 0.05 wt %. The two different types of hydrophilic nanoparticles were nano-structured fumed silica dispersions and colloidal silica. Three particle sizes were tested for each of the nanoparticle types, resulting in a total of six nanofluids used for analysis. The nano flooding was conducted as a tertiary EOR method after secondary water flooding. Interfacial tension and contact angle measurements were performed to better understand the mechanisms.

In the core flooding results, the fumed silica nanofluids performed better than the colloidal nanofluids, and additional oil recovery increased with increasing particle size. Differential pressure increased throughout the nano flooding stage, insinuating that nanoparticles are being retained in the core plugs, likely via log-jamming and/or mechanical entrapment. This is verified by analysis of the effluent nanofluid from the fumed silica core flooding tests. The IFT and contact angle measurements do not have clear trends corresponding to the core flooding results. These results suggest that mechanical mechanisms are driving the increase in oil recovery in this system, with only a minor contribution from chemical mechanisms. The mechanical log-jamming mechanism is likely the dominant mechanism in the system.

INTRODUCTION

As it has become more difficult to find new reservoirs for oil and gas production, the industry has shifted focus to researching ways to extract more hydrocarbons out of reservoirs already in production. Water flooding techniques have been employed in various ways for decades, but recently interest has been growing around using nanofluids (nanoparticles suspended in fluids) for a new enhanced oil recovery (EOR) technique.

A nanoparticle is defined as a particle with a size range of 1 nm to 100 nm. Rock pore channels are typically on the order of micrometers, so the nanoparticles can travel easily through a reservoir so long as they do not aggregate and/or agglomerate to form larger structures or adsorb unto the rock surface.

Previous studies have found that hydrophilic silica nanoparticles increase oil recovery[1,2,3,4]. Suggested mechanisms contributing to increased oil recovery include interfacial tension reduction, wettability alteration[5] (especially via an increase in structural disjoining pressure[6,7,8] and microscopic diversion[9]. The surface area to volume ratio can be very high for nanoparticles, enhancing the chemical reactivity of the nanofluid and resulting in the effect that fewer nanoparticles are needed to achieve similar functions of other EOR agents such as surfactants and polymers.

Hydrophilic silica nanoparticles and nano-structured particles are the focus of this study for three main reasons: 1) they have been shown to improve oil recovery in previous studies[1,2,3,4], 2) they are typically cheaper to manufacture and purchase compared to other nanoparticles such as titanium dioxide and 3) they are composed of over 99% silicon dioxide (SiO_2), which is the main component of sandstone, so they are environmentally friendly especially when compared with other chemical agents such as polymers.

The objective of this study is to determine the optimum nanoparticle based morphology and particle size for tertiary EOR using core flooding experiments. Interfacial tension (IFT) and contact angle measurements were conducted to attempt to shed light on the potential mechanisms contributing to the increase in oil recovery. A silica particle concentration of 0.05 wt% in the nanofluids was selected based on previous research[2] that identified that as the optimal concentration for a hydrophilic silica nanoparticle.

MATERIALS

Porous media

Water-wet Berea sandstone core plugs, with an average length of 13 cm and diameter of 3.8cm, were used for this study. The average porosity of the core plugs was 18.6% and the average permeability was 362 mD (Table 1. **Table of Berea sandstone properties.** The core plugs were cleaned using methanol via a soxhlet extraction apparatus at approximately 65 to 70 ^{o}C for 24 hours. After cleaning, they were placed in an oven set at 60 ^{o}C for over 48 hours. A Helium porosimeter and a constant head permeameter were used to measure porosity and permeability, respectively. The core plugs were saturated with reservoir brine (3 wt% NaCl) using a vacuum container (P ≈ 0.1 bar) for about 2

hours. They remained in the reservoir brine bath until they were used in the core flooding experiments. The original pore volume was determined by subtracting the dry weight of the core after cleaning from the wet weight of the core after it was saturated with the initial reservoir fluid. The cores were not aged in crude oil at any time during the experimental process, so it is assumed that they are water-wet and do not undergo a change in wettability during the duration of the experiments.

Table 1. Table of Berea sandstone properties.

Core #	Length (cm)	Diameter (cm)	Pore volume (mL)	Porosity (%)	Permeability (mD)
1	13.0	3.8	23.2	18.1	394
2	13.0	3.8	26.1	18.4	438
3	13.0	3.8	25.4	18.2	358
4	12.9	3.8	24.7	17.8	337
5	13.0	3.8	24.8	20.8	285
6	13.0	3.8	24.8	18.5	363
Average	13.0	3.8	24.8	18.6	362.2

X-ray diffraction (XRD) analyses were conducted for five sister samples taken from the same block as the core plugs used in this study. The results show that the majority of the sandstone is composed of quartz (silicon dioxide), with microcline and diopside as the secondary components (table 2).

Table 2. XRD mineral analysis of Berea core plugs (% mass).

Mineral	Sample					Average
	1	2	3	4	5	
Quartz	94.59	93.1	92.99	94.84	93.06	93.7
Microcline	3.94	5.67	5.65	4.07	5.62	5
Diopside	1.47	1.23	1.36	1.09	1.32	1.3

Fluids

A degassed crude oil from the North Sea was used for all experiments. It was filtered to 5 µm. The crude oil's properties are described in Tichelkamp et al. (2014), where it is referred to as "crude A". It has an API of 33.4 and its composition is 61.2 wt% saturates, 32.4 wt% aromatics, 4.9 wt% resins and 1.5 wt% asphaltenes.

A synthetic reservoir brine was mixed for the initial saturation of the core plugs prior to drainage. The synthetic reservoir brine was composed of 3.0 wt% sodium chloride (NaCl) and deionized water. A synthetic North Sea brine (NSB) was used as both the fluid for the water flooding stage of the core flooding experiments and as a base for the nanofluids. The NSB was made with a mixture of deionized water, sodium chloride,

sodium hydrogen carbonate, sodium sulfate, calcium chloride, magnesium chloride, strontium chloride and potassium chloride. This results in a salinity of 3.53%.

Nanofluids with concentrations of 20 wt% nanoparticles (NPs) suspended in deionized water with a stabilizer were provided by Evonik Industries. All of the concentrated nanofluids contained a sodium hydroxide stabilizer with the exception of the large colloidal nanofluid which contained a potassium based stabilizer. The concentrated nanofluids were then diluted to 2 wt% with deionized water and then further diluted to 0.05 wt% with the synthetic NSB. The "final" nanofluids were visually stable for at least 24 hours with the exception of the large colloidal nanofluid.

Six different nanofluids were mixed based on six different nanoparticles. All of the nanoparticles were hydrophilic, silica particles with primary particle diameters less than 100 nm (table 3). Three of the NPs were nano-structured silica particles produced via a pyrogenic (fumed) process with primary particle diameters ranging from 7 to 16 nm that form agglomerates with diameters in the range of 80 to greater than 110 nm. Fumed-L refers to the nanofluids composed of the largest fumed silica NPs (based on mean primary particle size), fumed-M refers to the medium sized particle and fumed-S refers to the smallest silica NPs. The other three nanofluids were made with colloidal silica NPs that are spherical particles with limited, if any, agglomeration. Their primary particle size is similar to the fumed silicas. Three different particle sizes were used for the colloidal silicas and named similarly to the fumed silica nanoparticles (colloidal-L, colloidal-M and colloidal-S). The colloidal silicas are less likely to form agglomerates than the nano-structured fumed silicas. This is due to their different surface properties as a result of their different manufacturing processes.

The densities of the brines and nanofluids were measured using a pycnometer, and the viscosities were measured using a rotating viscometer (table 4).

Table 3. Description of primary particle size and agglomerate size for the particles used in the six nanofluids. The naming convention (L, M, S) is based on the mean primary particle size. The particle size analyses were conducted using either static light scattering or dynamic light scattering methods based on the appropriate detection range. All of the particle size analyses were conducted with the silica dispersed in DI water.

Nanoparticle	Mean primary particle size (nm)	Median agglomerate particle size (nm)
Fumed-L	16	106
Fumed-M	10	81
Fumed-S	7	86
Colloidal-L	75	82
Colloidal-M	18	18
Colloidal-S	8	8

Table 4. Table of fluid properties.

Fluid	Density (g/cm^3)	Viscosity (cP)	Temperature (^oC)
Crude Oil	0.865	19.90[1]	20
Reservoir Brine	1.022	1.02	22.8
North Sea Brine	1.025	1.08	22.8
Fumed-L	1.025	1.02	22
Fumed-M	1.025	0.97	22.8
Fumed-S	1.022	0.94	22.8
Colloidal-L	1.023	0.91	20.4
Colloidal-M	1.025	1.02	20.7
Colloidal-S	1.023	0.97	22.8

[1]from Tichelkamp et al., 2014

EXPERIMENTAL SETUP

The core flooding apparatus is shown in figure 1. The system uses plastic piping with a diameter of 0.125 inches. The sleeve pressure in the Hassler core cell was set at 16 to 20 bar. All experiments were performed at ambient conditions. Effluent from the core cell was collected in 5 mL glass test tubes that were manually switched and recorded every 5 minutes. Manual pressure readings were also taken at these intervals.

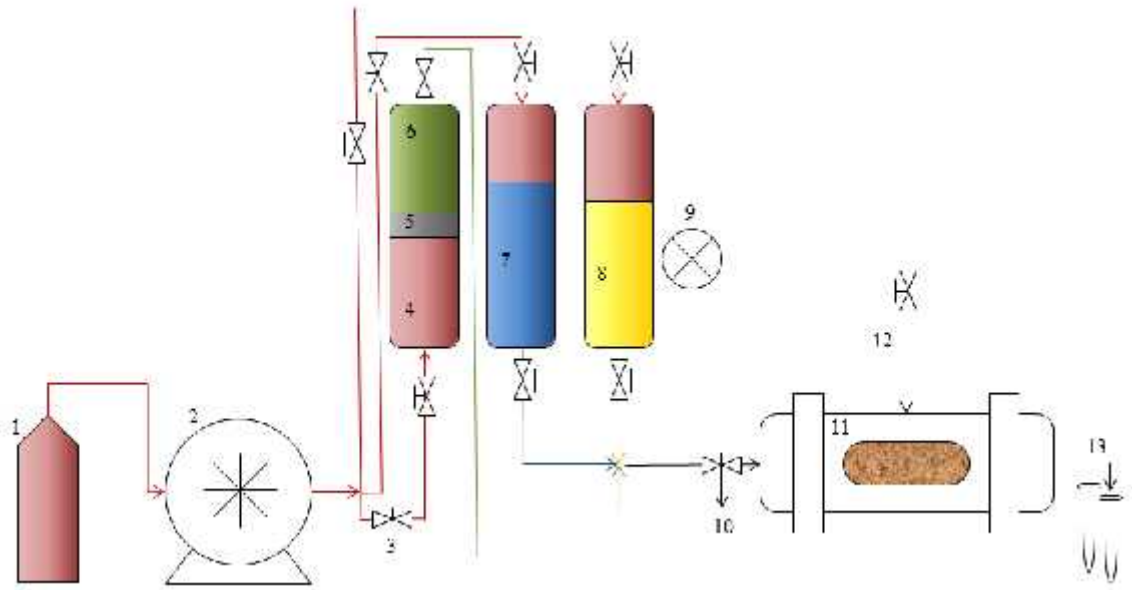

Figure 1. Experimental setup of the core flooding apparatus. 1) Exxol D60 pump fluid, 2) pump, 3) valves, 4) Exxol D60 displacing reservoir fluid, 5) piston to separate the oils, 6) crude oil, 7) NSB, 8) nanofluid, 9) pressure gauge, 10) bypass valve, 11) Hassler cell holder with core, 12) sleeve pressure, 13) effluent into test tubes.

EXPERIMENTAL PROCEDURE

Core flooding

1. The drainage process was conducted by injecting oil at 0.4 mL/min until it appeared that no more brine would be produced (typically after two pore volumes of total injection). This procedure established the initial water saturation.
2. Water flooding was then conducted with the synthetic North Sea brine to simulate imbibition conditions in the North Sea. The brine was injected at 0.4 mL/min until it appeared that no more oil would be produced by this method (typically after two pore volumes of total injection). This procedure determined the residual oil saturation.
3. Tertiary nanofluid flooding was then conducted at an injection rate of 0.4 mL/min until it appeared that no more oil would be produced by this method (typically after two pore volumes of total injection).
4. The oil recovery performance (expressed as the percent of the original oil in place - % OOIP) was evaluated for each core flooding experiment.

Interfacial tension (IFT)

The interfacial tension (IFT) was measured between the crude oil and the NSB and the crude oil and each nanofluid. A SVT20 spinning drop video tensiometer was used for the analyses. Rotation speed was kept at 4000 to 6000 rpm and temperature was held constant at 22.8 ^{o}C by a heating/cooling system. The experiments were conducted until it was obvious that the IFT had reached a stable value (typically after 1 to 2 hours of testing).

Contact angle

The contact angle of an oil droplet in the NSB and in each of the nanofluids was measured using the sessile drop technique. The oil droplet was suspended from a synthetic silica (glass) surface and surrounded by the testing liquid. Pictures were taken every 10 minutes over a 10 hour time frame to see if the contact angle stabilized over time. Measurements were conducted with a Goniometry KSV CAM instrument at ambient conditions.

RESULTS

Core flooding results

A total of six core flooding experiments were conducted: one for each nanofluid. The fumed silica nanofluids performed better than the colloidal nanofluids, and additional oil recovery increased with increasing particle size (figures 2 and 3). Differential pressure was recorded for each of the core flooding experiments (figures 4 and 5) and continually increased during each of the tertiary nano flooding stages. The results are summarized in table 5.

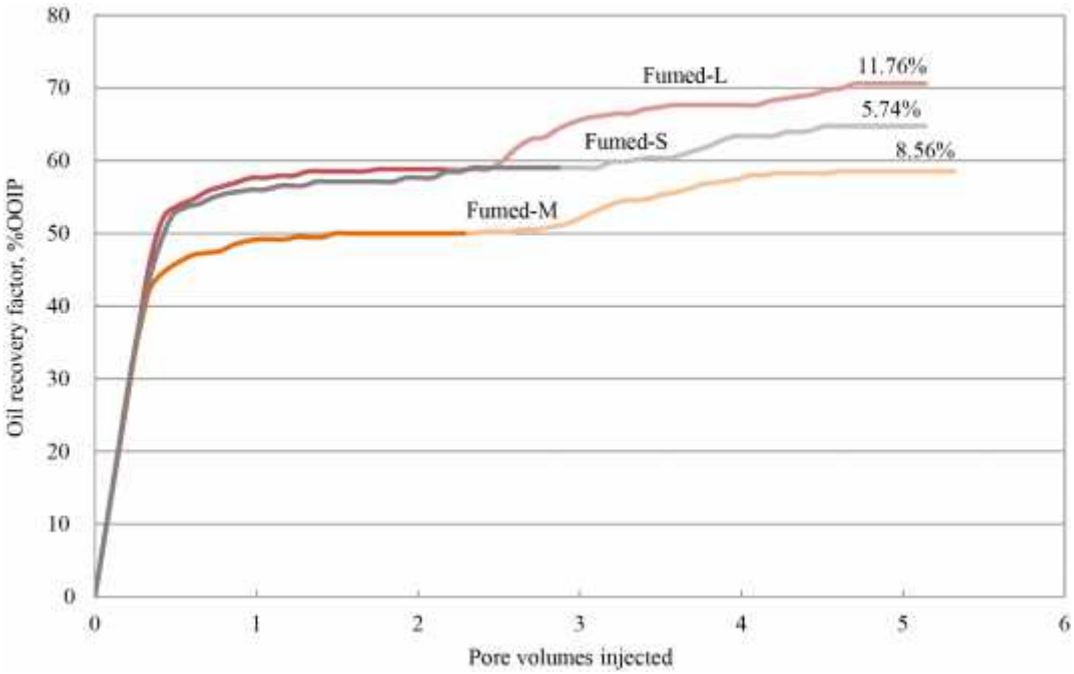

Figure 2. Core flooding results from the fumed NPs. The darker lines represent water flooding and the lighter lines represent nano flooding. The values are the %OOIP produced by the nano flooding alone.

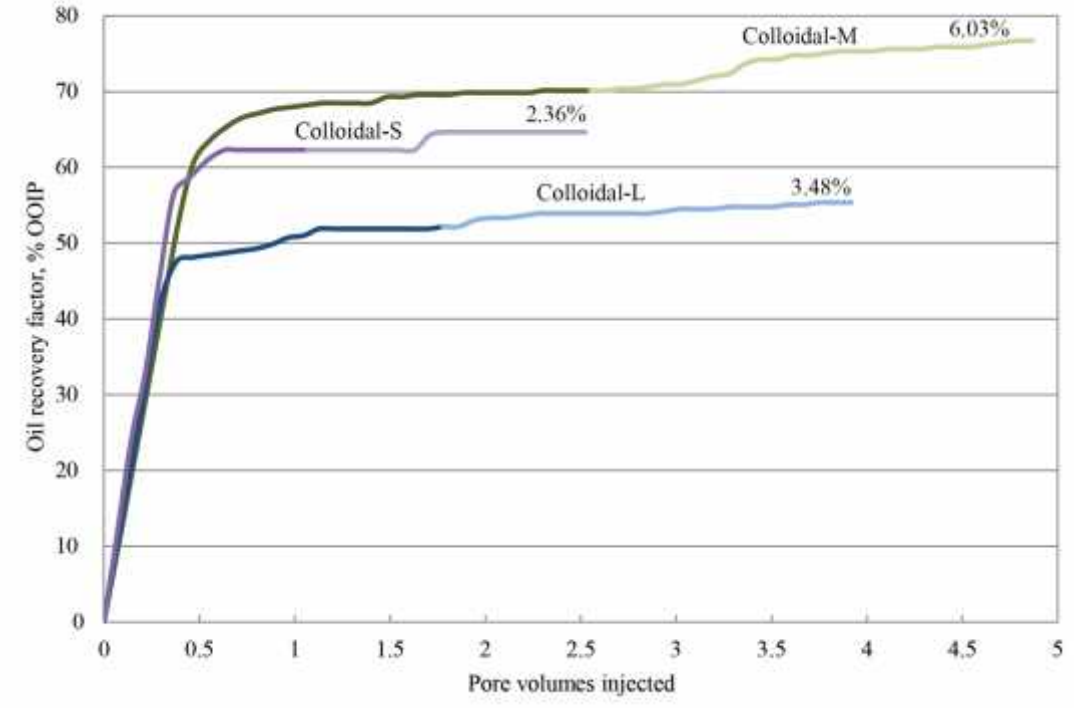

Figure 3. Core flooding results from the colloidal NPs. The darker lines represent water flooding and the lighter lines represent nano flooding. The values are the %OOIP produced by the nano flooding alone.

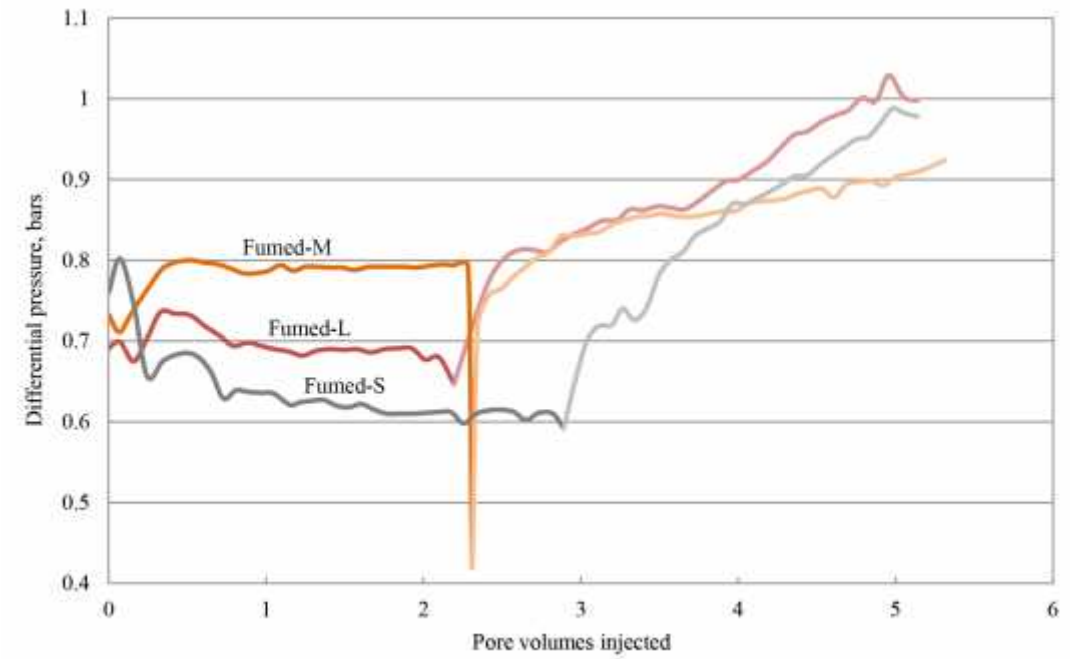

Figure 4. Differential pressure from the fumed NPs. The darker lines represent water flooding and the lighter lines represent nano flooding. The large pressure drop for the fumed-m test is from a short down time (< 2 min.) while switching fluid vessels.

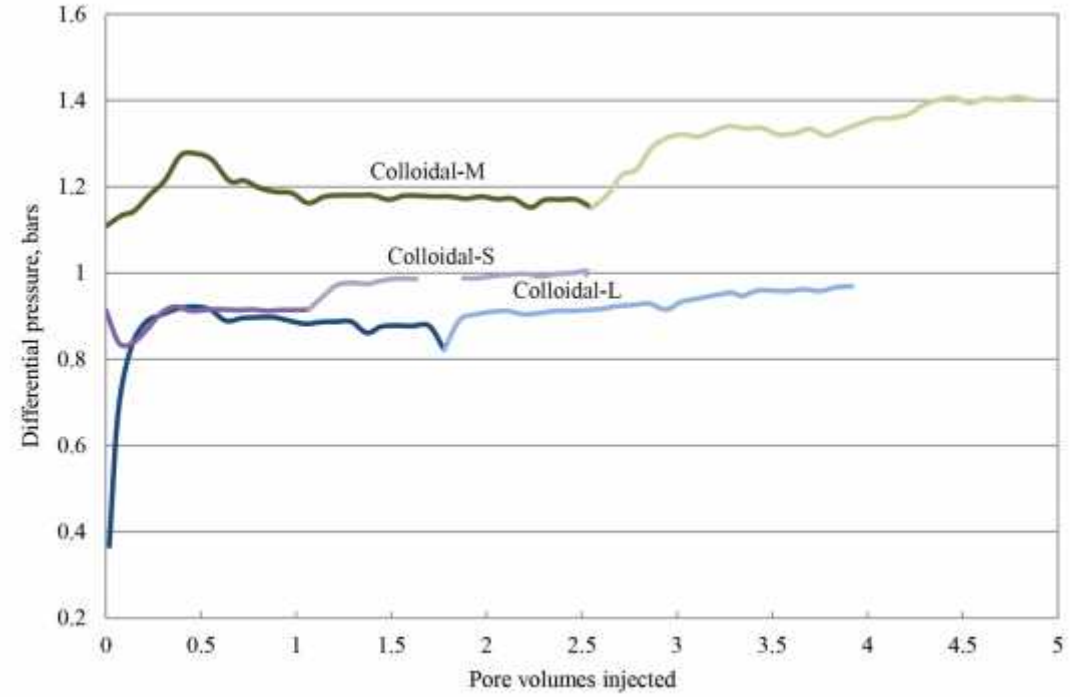

Figure 5. Differential pressure from the colloidal NPs. The darker lines represent water flooding and the lighter lines represent nano flooding.

Table 3. Summary of core flooding results.

Test #	Nanofluid	Core #	S_{wi}	S_{or}	% OOIP – water flooding	%OOIP – nano flooding	% increase from water to nano flooding
1	Fumed-L	1	0.27	0.30	58.82	11.76	20.00
2	Fumed-M	2	0.28	0.36	50.00	8.56	17.11
3	Fumed-S	3	0.28	0.29	59.02	5.74	9.72
4	Colloidal-L	4	0.30	0.34	52.17	3.48	6.67
5	Colloidal-M	5	0.26	0.22	70.14	6.03	8.59
6	Colloidal-S	6	0.40	0.23	62.29	2.36	3.78

IFT and contact angle

The IFT results show that the addition of NPs to the brine decreases the IFT (table 6). The fumed NPs have a greater IFT reduction than the colloidal NPs, but there is no clear trend correlating with the core flooding results. The contact angle measurements also have no clear trend correlating with the core flooding results.

Table 6. Summary of interfacial tension and contact angle results.

Fluid	IFT	Contact angle
NSB	16.41	153.4
Fumed-L	12.61	158.4
Fumed-M	11.96	160.6
Fumed-S	14.85	157.2
Colloidal-L	12.15	---
Colloidal-M	15.35	---
Colloidal-S	12.99	165.2

DISCUSSION

Based on the core flooding results, the fumed silica dispersions are a better choice for EOR applications than the colloidal silica. For both the fumed and colloidal NPs, there was a positive correlation between particle size and oil recovery. The larger the particle size, the larger the additional oil recovery. The fumed-S nanofluid is composed of the same nanoparticles Hendraningrat et al. (2013a) used in their studies. The results presented here are similar to their findings, where they observed a 5.32% and 4.69% increase in OOIP from the NPs equivalent to those used in the fumed-S nanofluid. This study achieved a 5.74% increase in OOIP for the comparable nanofluid. This serves as a validation point for the core flooding tests. However, more core flooding tests are needed to assess the repeatability and error margin for each nanofluid.

The IFT and contact angle measurements do not follow the same trends as the core flooding results. However, the IFT measurements do show that the fumed NPs have a greater average IFT reduction than the colloidal NPs. The IFT reduction mechanism likely plays a small role in the increase in oil recovery, but it cannot be the dominant mechanism. It is interesting to note that the larger the nanoparticle, the smaller the surface area to volume ratio, leading to a decrease in the ability to perform surface interactions. Because the larger, technically less chemically reactive, nanoparticles outperform their smaller counterparts, it appears that a mechanical, rather than a chemical, mechanism is the driver for enhanced oil recovery for this system.

Preliminary adsorption data from the core flooding effluent produced during the nano flooding stage indicate that the silica particles are retained within the core. Preliminary results from the nano flooding conducted with nano-structured particles display a trend where particle retention inside the core increases with particle size (i.e. the fumed-L nano flooding has the smallest concentration of silica in the effluent and the fumed-S nano flooding has the largest concentration of silica in the effluent). Nano-structured particle concentration in the effluent also increases over time.

In addition, the increase in differential pressure throughout the nano flooding stage also insinuates that nanoparticles are being retained within the core plug. This is more likely due to mechanical mechanisms such as log-jamming (as introduced by Bolandtaba et al., 2009) of the silica particles within pore throats and less likely from chemical mechanisms such as adsorption unto the rock surface.

A schematic illustrating the log-jamming mechanism can be found in figure 6. This could be the dominant mechanism in the system based on 1) the increase of oil recovery as particle size increases, insinuating the recovery mechanism is mechanical in nature, 2) the decreased concentration of NPs in the core flooding effluent, proving that NPs are being retained within the system, 3) the increase in differential pressure throughout the nano flooding stage.

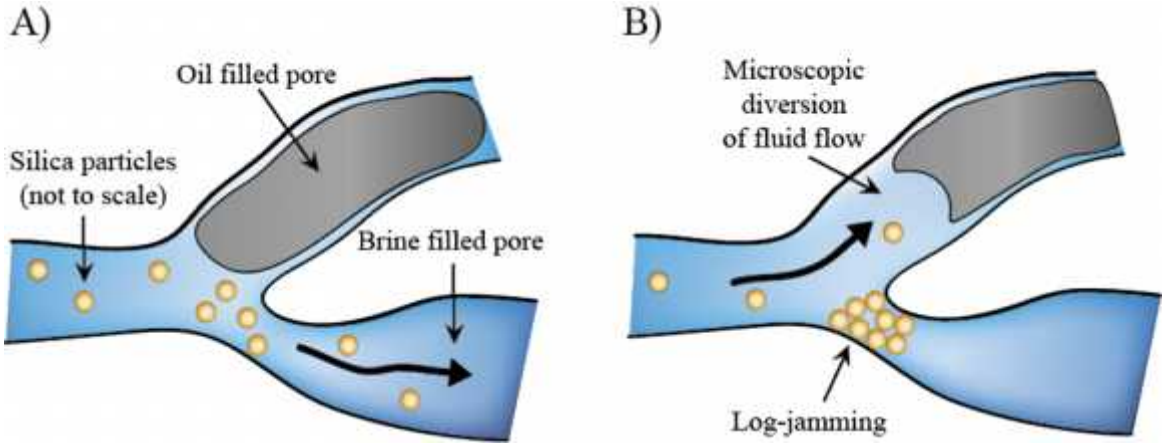

Figure 6. An interpretation of the log-jamming mechanical mechanism leading to microscopic diversion of the fluid flow and subsequent additional oil recovery. A) The nanofluid initially flows along the path of least resistance. Oil in untouched pores provides resistance to brine and nanofluid sweeps because of its higher fluid viscosity. B) Eventually, the silica particles may block a previously available pore throat. This is especially likely if there is a constriction in the pore diameter, causing the particles to crowd together as they attempt to squeeze through the opening. This could lead to nanoparticles creating a relatively impassable wall via a process called "log-jamming". This would cause the injected fluid to be diverted to the other pore throats. The increase in pressure as a result of decreased permeability would allow the fluid to overcome the force needed to mobilize the viscous oil.

The cations in the NSB and the alkaline stabilizers in the nanofluids have influence over the results, but the specific impact is currently being investigated and is beyond the scope of this paper.

CONCLUSIONS

1. Fumed silica dispersions are more promising than colloidal silica nanoparticles for enhanced oil recovery.
2. Oil recovery increases with increasing nanoparticle diameter for the nanofluids analyzed in this study.
3. Mechanical mechanisms are driving the increase in oil recovery, with maybe a minor contribution from chemical mechanisms.
4. The log-jamming mechanism is likely the dominant mechanism in the system.
5. More research is needed to better understand the mechanisms behind the increase in oil recovery from nano flooding. Also, more core flooding tests are needed to check the repeatability and error margin of the results presented in this paper.

ACKNOWLEDGEMENTS

Thank you to Evonik Industries AG for providing the nanofluids, adsorption analysis, North Sea brine recipe, and advice. Thank you to NTNU laboratory engineer Roger Overå for assistance.

REFERENCES

1. Hendraningrat, L., Li, S. and Torsæter, O., 2013a, A coreflood investigation of nanofluid enhanced oil recovery in low-medium permeability Berea sandstone. Paper SPE 164106 presented at the SPE International Symposium on Oilfield Chemistry held in the Woodlands, Texas, USA, 8 – 10 April 2013, 14 p.

2. Hendraningrat, L., Li, S. and Torsæter, O., 2013b, Enhancing Oil Recovery of Low-Permeability Berea Standstone through Optimized Nanofluids Concentration. Paper SPE 165283 presented at the SPE Enhanced Oil Recovery Conference held in Kuala Lumpur, Malaysia, 2 – 4 July 2013, 10 p.

3. Ju, B., Tailiang, F. and Mingxue, M., 2006, Enhanced oil recovery by flooding with hydrophilic nanoparticles, *China Particuology* **4**: 41-46.

4. Roustaei, A., Saffarzadeh, S. and Mohammadi, M., 2013, An evaluation of modified silica nanoparticles' efficiency in enhancing oil recovery of light and intermediate oil reservoirs. *Egyption Journal of Petroleum* **22** (3): 427–433.

5. Li, S., Kaasa, A.T., Hendraningrat, L. and Torsæter, O., 2013, Effect of silica nanoparticles adsorption on the wettability index of Berea sandstone. Paper SCA2013-059 presented at the international symposium of the Society of Core Analysts held in Napa Valley, California, USA, 16–19 September 2013, 6 p.

6. Chengara, A., Nikolov, A. D., Wasan, D. T., Trokhymchuk, A. and Henderson, D., 2004, Spreading of nanfluids driven by the structural disjoining pressure gradient. *Journal of Colloid and Interfacial Science* **280**:192-201.

7. Wasan, D.T. and Nikolov, A., 2003, Spreading of nanofluids on solids, *Nature* **423**: 156-159.

8. Wasan, D.T., Nikolov, A. and Kondiparty, K., 2011, The wetting and spreading of nanofluids on solids: role of the structural disjoining pressure, *Curr Opin Colloid Interface Sci* **16**: 344-349.

9. Skauge, T., Hetland, S., Spildo, K. and Skauge, A., 2010, Nano-sized particles for EOR, Paper SPE 129933, presented at the SPE Improved Oil Recovery Symposium held in Tulsa, Oklahoma, USA, 24-28 April 2010, 10 p.

10. Tichelkamp, T., Vu, Y., Nourani, M. and Øye, G., 2014, Interfacial tension between low salinity solutions of sulfonate surfactants and crude and model oils, *Energy Fuels* **28**: 2408 – 2414.

11. Bolandtaba, A.F., Skauge, A. and MacKay, E., 2009, Pore scale modeling of linked polymer solution (LPS) – A new EOR process, presented at the 15th European Symposium on Improved Oil Recovery, Paris, France, April 27-29, 2009. 17 p.